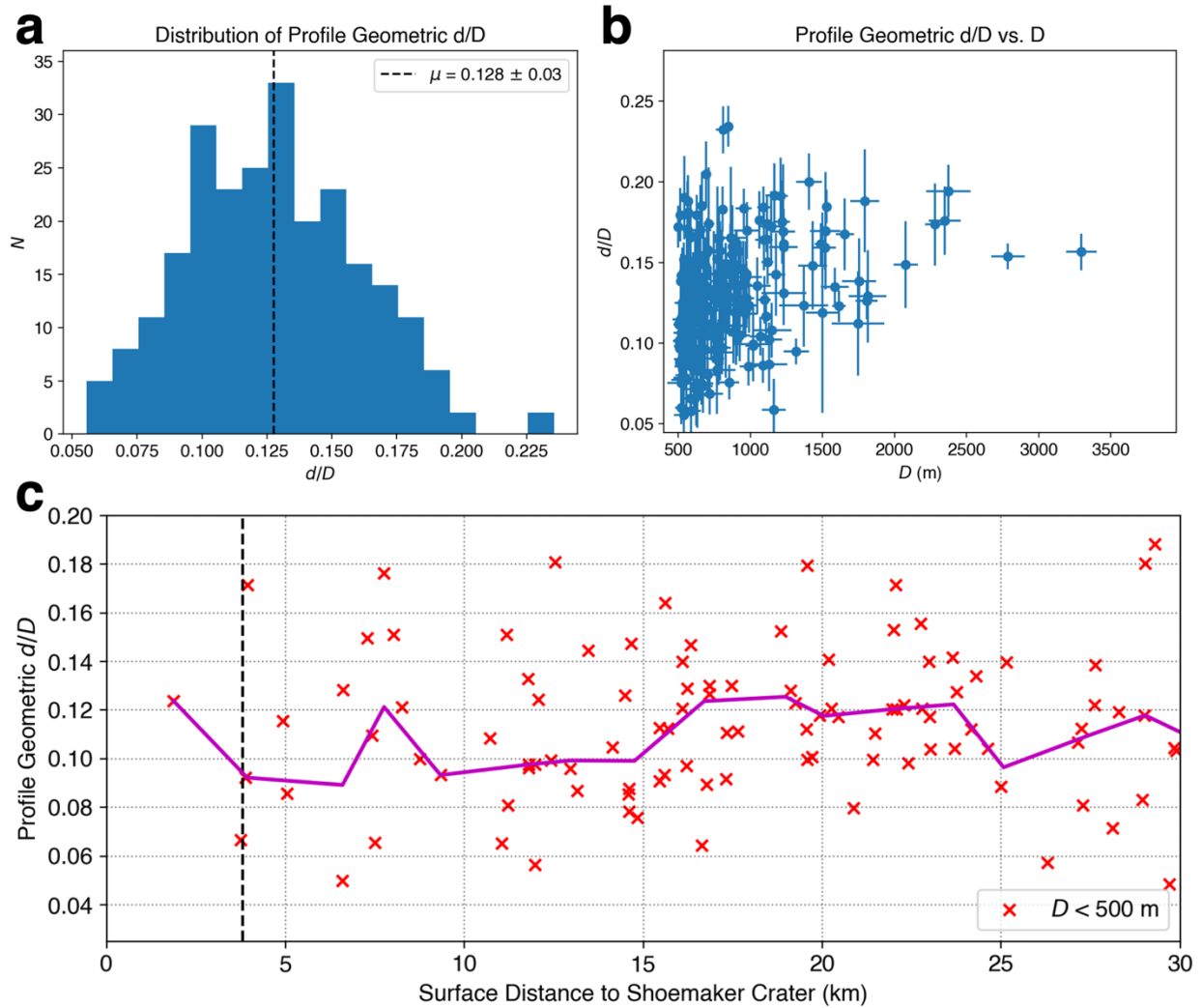
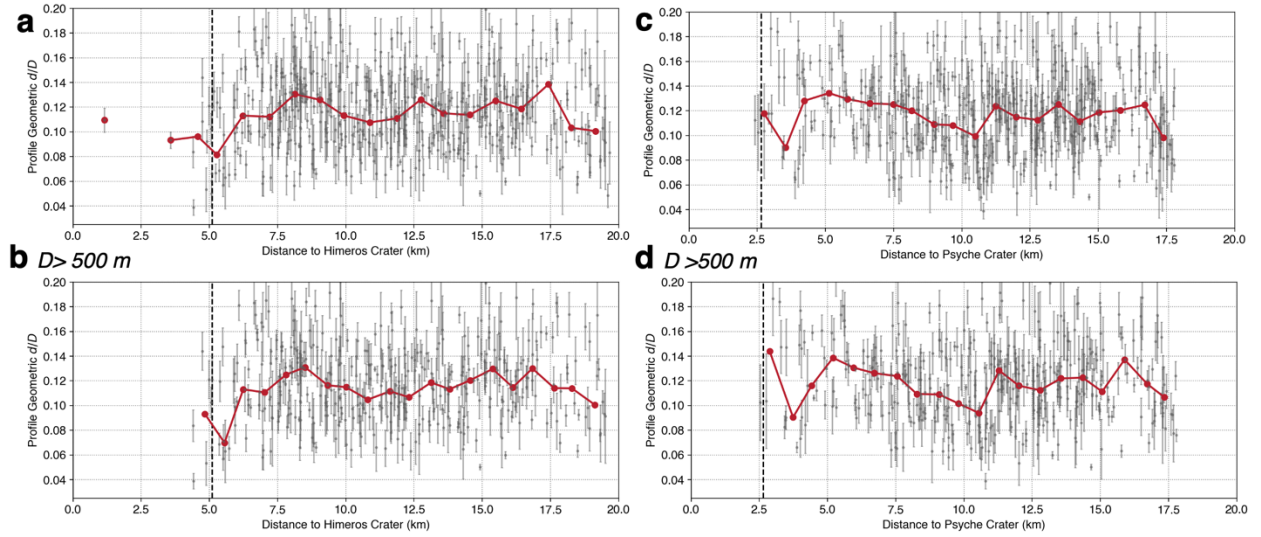


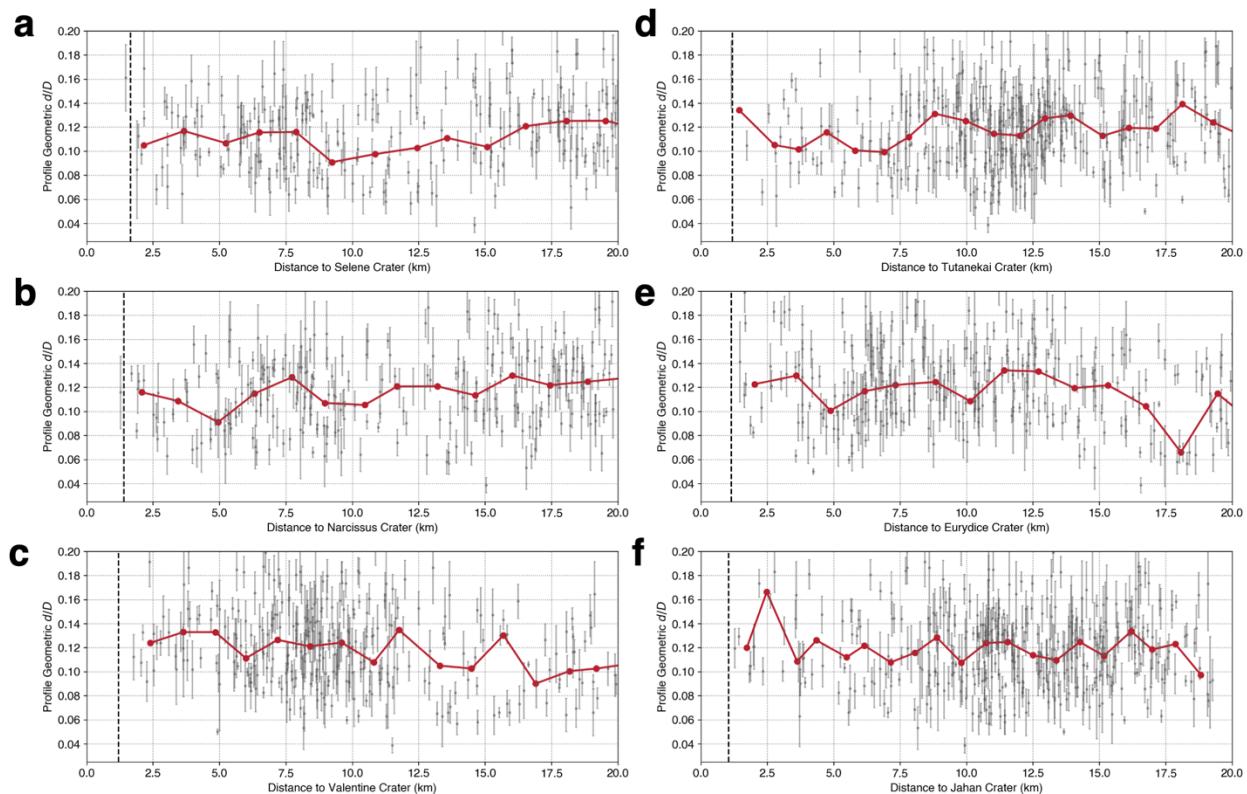
Extended Data



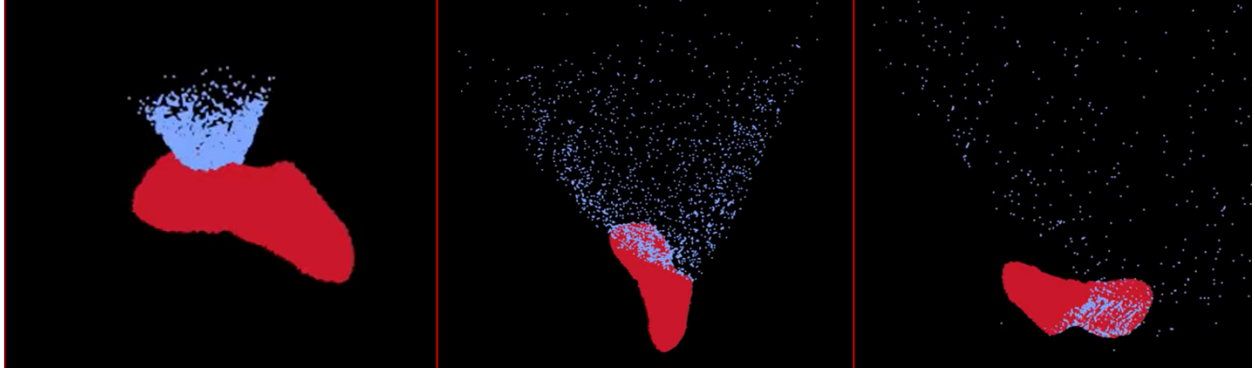
Extended Data Figure 1. **a**, Histogram showing the global distribution of crater depth, d , to diameter, D , ratio, d/D . The d/D of craters on Eros have a mean value of 0.128 and standard deviation of 0.03, but deviate from a normal distribution. **b**, The distribution of crater d/D as a function of D . There is a larger spread in d/D values at smaller sizes, and craters 500–1000 m in diameter exhibit the largest degree of degradation. **c**, The d/D of craters with $D < 500$ m (red crosses) as a function of surface distance to Shoemaker. The magenta curve shows the moving average (median) of the red crosses. No clear trend exists for smaller ($D < 500$ m) craters compared to larger craters (Fig. 2a).



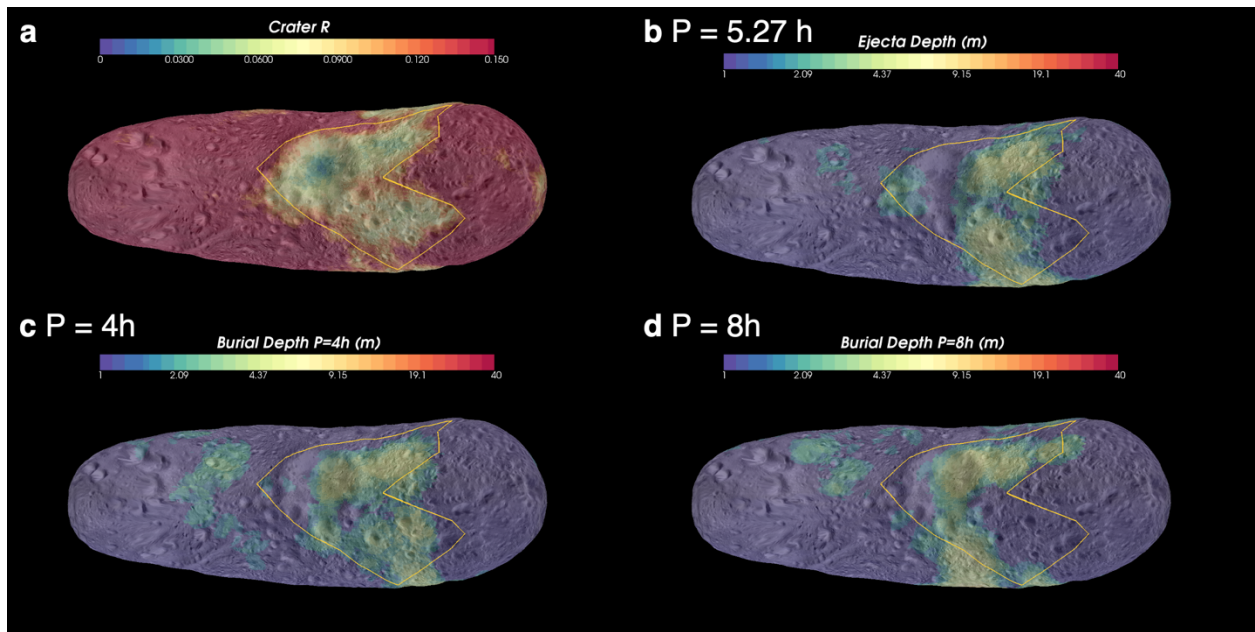
Extended Data Figure 2. Crater geometric height d/D (grey circles) as a function of distance to other two largest craters on Eros, Himeros crater ($D = 10.2$ km) and Psyche crater ($D = 5.2$ km). The red curve in each panel shows the moving average (median) of the grey circles. The vertical black dashed line marks one crater radius. Unlike Shoemaker crater, no trends between d/D and distance to the other craters are apparent. **a**, d/D of all craters as a function of distance to Himeros crater. **b**, d/D of craters with $D > 500$ m, as a function of distance to Himeros crater. **c**, d/D of all craters as a function of distance to Psyche crater. **d**, d/D of craters with $D > 500$ m, as a function of distance to Psyche crater.



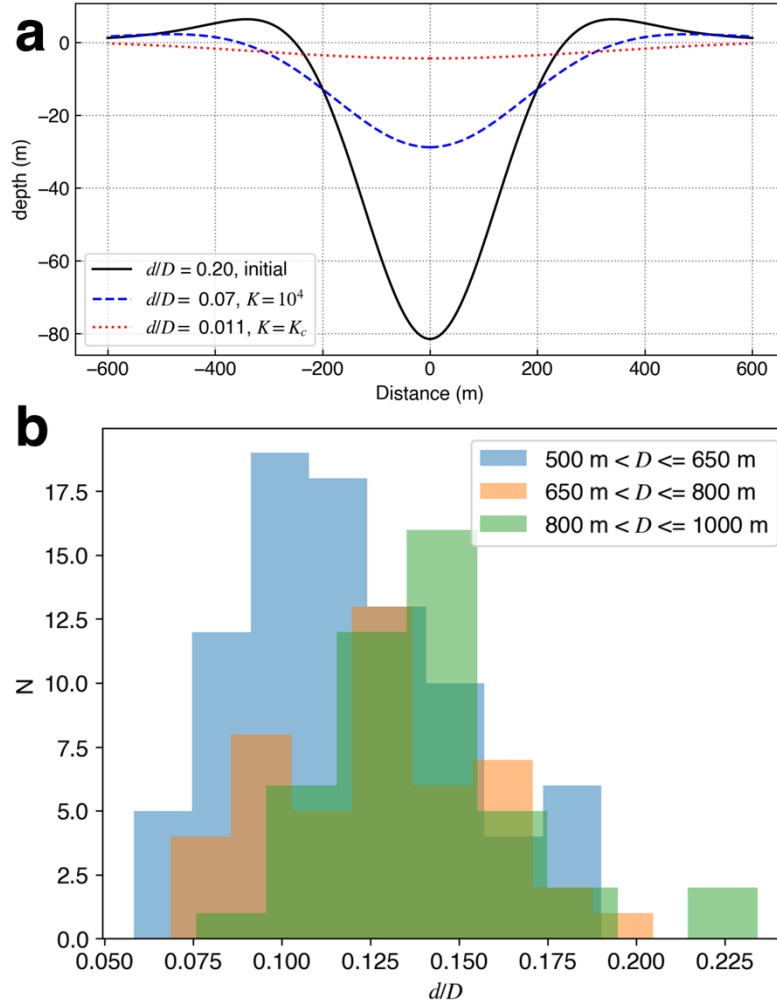
Extended Data Figure 3. Crater geometric height d/D (grey circles) of craters with $D > 500$ m as a function of distance to other large craters with $D > 2$ km on Eros. The red curve in each panel shows the moving average (median) of the grey circles. The vertical black dashed line marks one crater radius. Unlike Shoemaker crater, no trends between d/D and distance to the craters are apparent. d/D is shown as a function of distance to **a**, Selene crater, **b**, Narcissus crater, **c**, Valentine crater, **d**, Tutanekai crater, **e**, Eurydice crater, and **f**, Jahan crater.



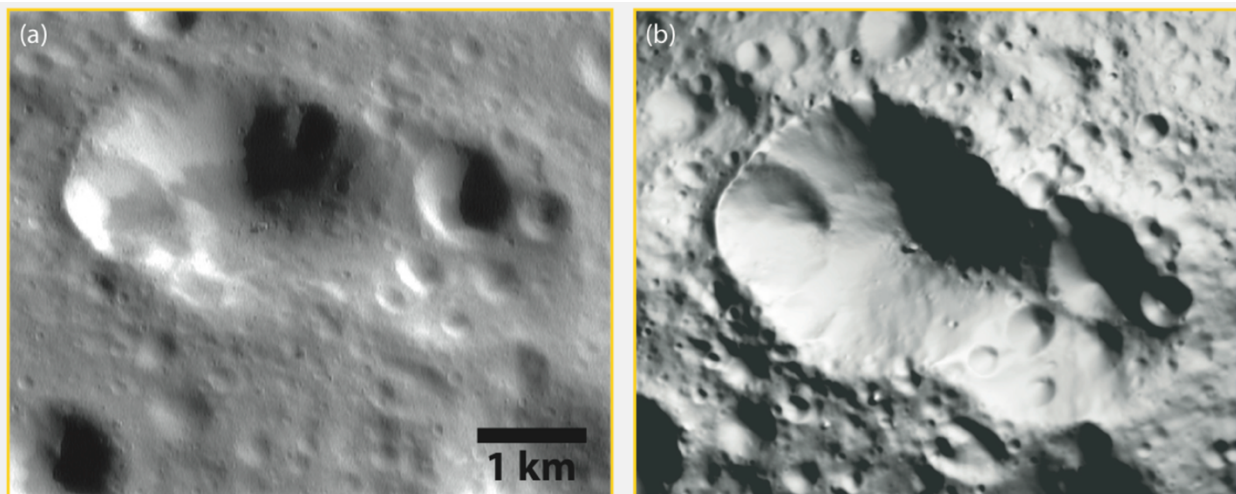
Extended Data Figure 4. Snapshots of a *pkdgrav* simulation (Case #1, see Extended Data Table 1) showing the evolution of ejecta (blue dots) and its re-impact on to a *pkdgrav* model of Eros (red rigid body), over the course of 0.5 an orbital period (2.7 h). Blue regions in the right panel show the re-impact points of ejecta on Eros.



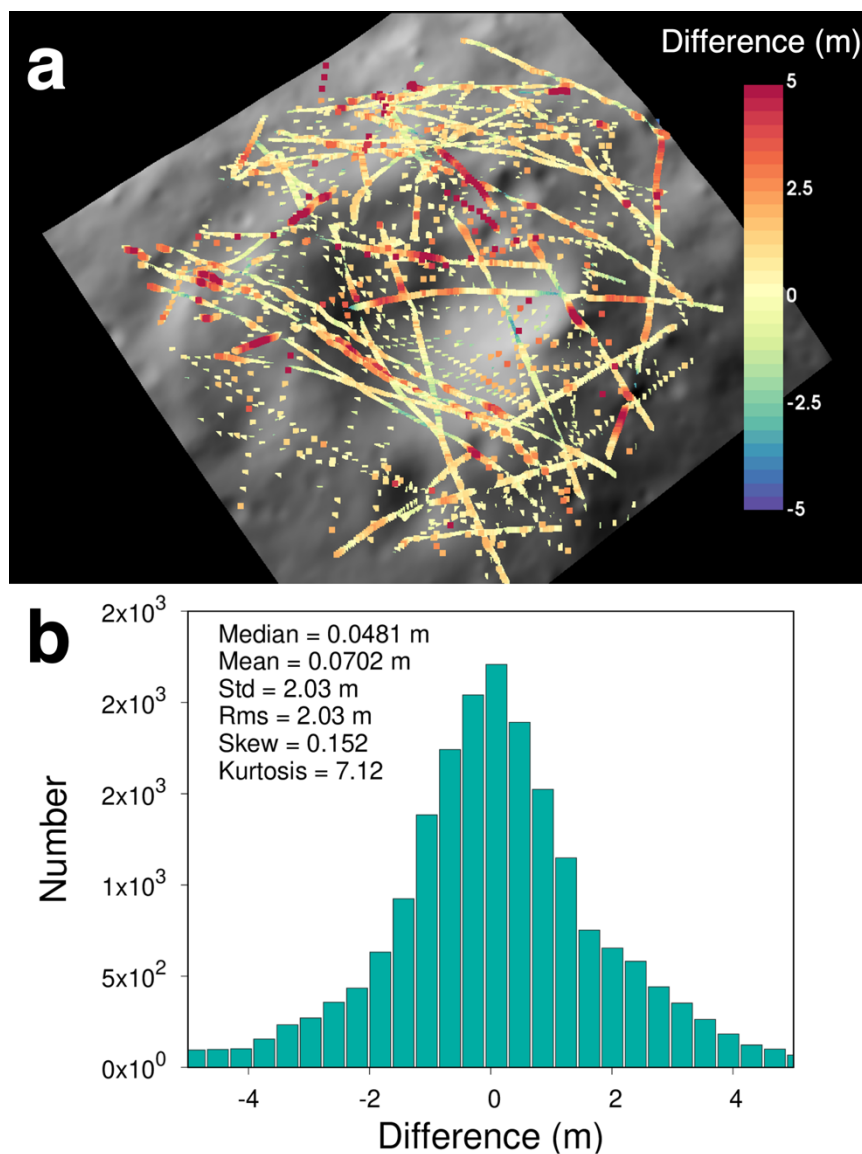
Extended Data Figure 5. Crater R and simulated ejecta depth for cases with variable Eros rotation periods, P , projected onto an Eros shape model using the SBMT shown with a projected basemap of Eros. The Shoemaker antipode is shown in each panel, highlighting the arrow shaped region (mapped as a yellow polygon in SBMT) of crater depletion. **a**, Crater R for craters with $D = 0.177 - 1$ km. **b**, outcome of *pkdgrav* simulation of ejecta deposition for a case where Eros had its current spin period, $P = 5.27$ h. **c**, **d**, similar to **b** except for $P = 4$ h and 8h, respectively. For all simulation cases, the ejecta that is deposited in the antipode is mostly concentrated within the arrow-shaped region. The $P=5.27$ h case has the closest qualitative match to the crater R pattern.



Extended Data Figure 6. a, Demonstration of crater degradation using the technique described in Methods Sec. 3. A fresh crater profile with $d/D = 0.2$ (black solid curve) is generated using Eq. (2) for a $D = 500$ m crater. The degradation of the crater can be modeled using Eq. (3) by applying different values of the downslope diffusion value, K . Example cases for mobilized height, $h = 1$, are shown that leads to $d/D = 0.07$ (blue dashed curve) for $K = 10^4$ and $d/D = 0.011$ (red dotted curve) for $K = K_c$, the critical downslope diffusion value for effective crater erasure (Eq. 4). **b**, The distribution of d/D for craters outside of the *Shallow Crater Region*. The mean d/D of craters gradually increases as a function of D for the sub-populations shown here: blue region shows craters with $D = 500 - 650$ m (mean $d/D = 0.117 \pm 0.03$), orange region shows craters with $D = 650-800$ m (mean $d/D = 0.127 \pm 0.03$), green region shows craters with $D = 800 - 1000$ m (mean $d/D = 0.14 \pm 0.03$).



Extended Data Figure 7. A comparison of **a**, an MSI image and **b**, the SPC DTM of the 2.3-km diameter crater Eurydice.



Extended Data Figure 8. Example of the verification of SPC DTMs of an Eros crater with NLR data. **a**, NLR tracks are used to create an NLR DTM for Bovary crater to compare against the SPC DTM of Bovary Crater. Colors of NLR data denote NLR DTM – SPC DTM residuals. **b**, Distribution NLR DTM – SPC DTM residuals with a root mean square (RMS) of 2.03 m.

Case	μ_e	P (h)	f_{ret}	V_{ret} (km ³)
1	0.35	5.27	0.35	5.72
2	0.41	5.27	0.41	6.67
3	0.55	5.27	0.54	8.73
4	0.41	-	0.45	7.26
5	0.41	4	0.40	6.47
6	0.41	8	0.43	6.94

Extended Data Table 1. Summary of *pkdgrav* ejecta deposition simulation cases and outcomes. The ejection scaling parameter, μ_e , was varied between 0.35-0.55, with a nominal value of 0.41. P = rotation period, f_{ret} = fraction of escaped ejecta, V_{ret} = volume of retained ejecta.

Crater	Mean Differences (m)	NLR-SPC DTM Residual (m)	NLR DTM -SPC DTM residual (m)
Bovary	0.07	2.03	2.18
CRT037	-0.06	2.31	2.19
CRT052	0.04	1.62	3.57
CRT068	0.03	1.7	2.87
CRT121	0.02	1.76	2.18
Mean	0.02	1.9	2.6

Extended Data Table 2. Summary of SPC verification using NLR. The mean values of each column are presented in the last row